

Localized structures in broad area VCSELs: experiments and delay-induced motion

Mustapha Tlidi, Etienne Averlant, Andrei Vladimirov, Alexander Pimenov,
Svetlana Gurevich and Krassimir Panayotov

Abstract We investigate the space-time dynamics of a Vertical-Cavity Surface-Emitting Laser (VCSEL) subject to optical injection and to delay feedback control. Apart from their technological advantages, broad area VCSELs allow creating localized light structures (LSs). Such LSs, often called Cavity Solitons, have been proposed to be used in information processing, device characterization, and others. After a brief description of the experimental setup, we present experimental evidence of stationary LSs. We then theoretically describe this system using a mean field model. We perform a real order parameter description close to the nascent bistability and close to large wavelength pattern forming regime. We theoretically characterize the LS snaking bifurcation diagram in this framework. The main body of this chapter is devoted to theoretical investigations on the time-delayed feedback control of LSs in VCSELs. The feedback induces a spontaneous motion of the LSs, which we characterize by computing the velocity and the threshold associated with such motion. In the nascent bistability regime, the motion threshold and the velocity

Mustapha Tlidi
Faculté des Sciences de l'Université libre de Bruxelles, Belgium e-mail: mtlidi@ulb.ac.be

Etienne Averlant
Faculté des Sciences de l'Université libre de Bruxelles, Belgium and IR-TONA, Vrije Universiteit
Brussel, Belgium e-mail: eaverlan@ulb.ac.be

Andrei Vladimirov
Weierstrass Institut for applied physics und stochastics, Berlin, Germany e-mail: vladimir@
wias-berlin.de

Alexander Pimenov
Weierstrass Institut for applied physics und stochastics, Berlin, Germany e-mail: Alexander.
Pimenov@wias-berlin.de

Svetlana Gurevich
Institut für theoretische Physik, Münster, Germany e-mail: gurevics@uni-muenster.de

Krassimir Panayotov
IR-TONA, Vrije Universiteit Brussel, Belgium and Institute of solid State physics, Sofia, Bulgaria
e-mail: kpanajot@b-phot.org

of moving LSs depend only on the feedback parameters. However, when considering the previously introduced mean-field model, theoretical predictions indicate that both motion threshold and velocity are strongly affected by the phase of the delay and by the carrier relaxation rate.

1 Introduction

Spontaneous symmetry breaking and self-organization phenomena have been observed in various fields of nonlinear science such as nonlinear optics, fibre optics, fluid mechanics, granular matter or plant ecology. The link between the well known Turing instability and transverse patterns formation in nonlinear optics was established for the first time by Lugiato and Lefever [1]. In their seminal paper, they considered an optical resonator filled with a passive nonlinear medium and driven by a coherent radiation beam. Since then, many driven systems have proven to allow periodic patterns in the transverse section of their output beam. Besides a periodic distribution of light, LSs may form in the plane perpendicular to the propagation axis. They are often called localized spots and localized patterns, or cavity solitons which appear either isolated, randomly distributed or self-organized in clusters forming a well-defined spatial pattern [2, 3]. When LSs are sufficiently separated from each other, localized peaks are independent and randomly distributed in space. However, when the distance between peaks decreases they start to interact via their oscillating, exponentially decaying tails [4, 5, 6, 7]. LSs have been reported in nonlinear resonators such as lasers with saturable absorbers [8, 9, 10], in passive nonlinear resonators [2, 3, 11], optical parametric oscillators [12, 13], in left-handed materials [14, 15, 16, 17], in exciton-polariton patterns in semiconductor microcavities [18, 19] and in the framework of the Ginzburg-Landau equation [20, 21, 22, 23, 24]. Phase solitons have been demonstrated far from any pattern forming instability [25, 26, 27, 28, 29, 30].

Localized structures are homoclinic solutions (solitary or stationary pulses) of partial differential equations. The conditions under which LSs and periodic patterns appear are closely related. Typically, when the Turing instability becomes subcritical, there exists a pinning domain where LSs are stable. This is a universal phenomenon and a well-documented issue in various fields of nonlinear science. The experimental observation of LSs in driven nonlinear optical cavities has further motivated the interest in this field of research. In particular, LSs could be used as bits for information storage and processing. Several overviews have been published on this active area of research [31, 9, 32, 33, 34, 35, 36, 37, 38, 39, 40, 41, 42, 43, 44, 45, 46, 47, 48].

Many theoretical and experimental studies on LS formation in VCSELs have been realized [49, 50]. They have been experimentally observed in broad area VCSELs both below [49, 51] and above [52] the lasing threshold when injecting a holding beam with appropriate frequency and power. A spatially LS has also been found in a medium size VCSEL, but only by using its particular polarization proper-

ties [53]. Cavity soliton lasers (CSLs) in a VCSEL system without a holding beam have been demonstrated both experimentally [54] and theoretically [55] in VCSELs subject to frequency selective optical feedback and in face to face coupled VCSELs [56, 57]. In these systems, the VCSELs are placed in self imaging optical systems with either an external grating or another VCSEL biased below lasing threshold, so that the system becomes bistable. Lasing spots spontaneously appear in these systems and can be switched on and off by another laser beam. As a matter of fact a broad area VCSEL with saturable absorber has been the first system in which LSs have been predicted and studied theoretically [58, 59, 60]. LSs in a monolithic optically pumped VCSEL with a saturable absorber have been demonstrated in [61] and their switching dynamics studied in [62]. Several applications of LSs in VCSELs have been demonstrated: optical memory [63], optical delay line [64] and optical microscopy [50].

In this chapter, we investigate the formation of LSs in Vertical-Cavity Surface-Emitting Lasers (VCSELs) subject to both optical injection and delay feedback control. These lasers are characterized by a large Fresnel number and a short cavity. VCSELs are the best candidate for localized structures formation in their transverse section. The first VCSELs were fabricated in 1979 [65] and later on they reached performances comparable to those of edge-emitting lasers [66, 67]. Nowadays VCSELs are replacing edge-emitting lasers in short and medium distance optical communication links thanks to their inherent advantages: much smaller dimensions, circular beam shape that facilitates coupling to optical fibres, two-dimensional array integration and on wafer testing that brings down the production cost [67]. As VCSELs emit light perpendicular to the surface and the active quantum wells, their cavity length is of the order of $1 \mu\text{m}$ - the wavelength of the generated light. Thanks to the maturity of the semiconductor technology VCSELs can be made homogeneous over a size of hundreds of μms while the characteristic LS size is about $10 \mu\text{m}$. The timescales of the semiconductor laser dynamics and LS formation are in the ns scale, which allows for fast and accurate gathering of data. Finally, VCSEL physics and dynamics are quite well understood [67, 68, 69].

We investigate experimentally and theoretically the formation of stationary LSs in VCSELs and we describe theoretically the effect of a time delayed feedback on the stability of LSs. For this purpose, we adopt the Rosanov-Lang-Kobayashi approach for modelling of delay feedback [70, 71].

This chapter is organized as follows. After an introduction, we provide a description of the VCSELs in Sec (2), the experimental setup and the observation of localized structures in a medium size VCSEL are described in Sec. (3). A theoretical description based on mean field model and the derivation of the generalized Swift-Hohenberg equation are given in Sec. (4). Stationary LSs and their bifurcation diagram are presented in Sec. (5). LSs brought into motion under the effect of delay feedback are discussed in Sec. (6). We conclude and draw some perspectives of the present work in Sec. (7).

2 Vertical-Cavity Surface-Emitting Lasers

The structure of a VCSEL is by far more complex than the one of an edge-emitting semiconductor laser. But this complexity, and the inherent fabrication costs, did not keep VCSELs from becoming the second most produced laser type [72, 73, 74]. The biggest advantages of this structure are the circular emission pattern and low divergence, which allow to easily couple the light to an optical fibre for optical interconnects. Moreover, the high reflectivity of the Bragg mirrors provide a low lasing threshold, which makes VCSELs the choice lasers for low power applications (such as optical mice for example). For high power applications, VCSELs can easily be coupled into arrays [75], which provides a high power coherent low divergence beam.

The emission surface of a VCSEL can be made from a few μm to some 200 μm - the first ones are best suited for low power applications, whereas the second category is typically used for spectroscopy. Apart of their use in spectroscopy, broad area VCSELs are best suited for LSs studies. They have several characteristics that makes them a choice material:

- Their use in information technologies provides a mastering of the fabrication process, leading to à la carte properties;
- The response time is much faster than the one in liquid crystals or photorefractive media, which makes them more likely to be used in potential high speed applications;
- Experiments can be carried out on a single one hundred micrometer chip, in comparison with some meter needed for creating LSs in gas cells;

The broad-area bottom emitting VCSEL structure we use in our experiments is described in Fig. 1. The top and bottom distributed Bragg reflectors consist of 30 and 20.5 $\text{Al}_{0.88}\text{Ga}_{0.12}\text{As}$ -GaAs layer pairs, respectively. The active region consists of three $\text{In}_{0.2}\text{Ga}_{0.8}\text{As}$ quantum wells embedded in GaAs barriers and AlGaAs cladding layers[75]. The bottom-emitting configuration allows the stand-alone VCSEL to have a better (more homogeneous) current distribution in the transverse plane and, therefore, is more suitable for producing LSs. Moreover a heat sink can be directly mounted on top of the p -contact and the p -doped DBR, which is the main source of heat. The temperature distribution is hence more homogeneous as well.

3 Experimental observations

3.1 Description of the experimental setup

The experimental setup used for the generation of two-dimensional LSs is shown in Fig. 2. The injection part consists of a tunable External Cavity Diode Laser (Master) in a Littrow configuration, optically isolated from the rest of the experiment. The

Fig. 1 View of a bottom-emitting VCSEL. The blue and green layers constitute the pairs in the Bragg mirrors. The red element is the cavity containing the quantum wells. The grey part is the substrate on which the structure has been grown and through which the light is emitted.

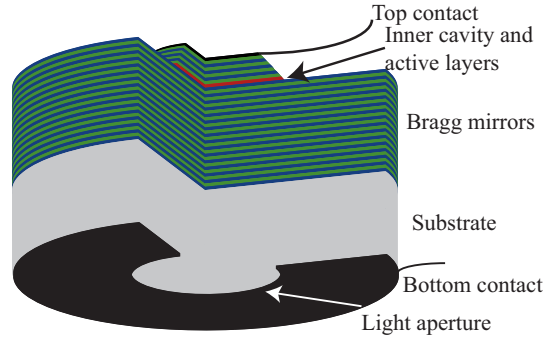
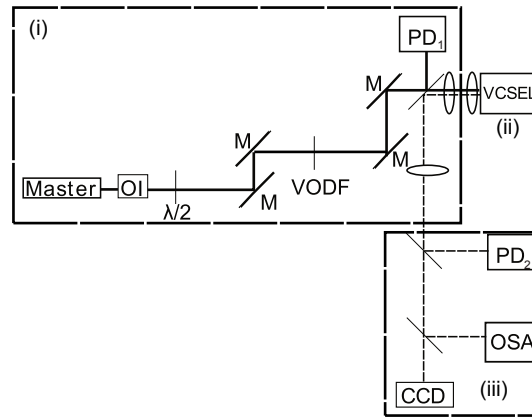


Fig. 2 Experimental setup schematic. The full line is the path of the light from the master laser, whereas the dashed line is the path followed by the light from the VCSEL. (i): injection preparation and monitoring; Master: master laser, OI: optical isolator, $\lambda/2$: half wave plate, M: mirror, VODF: variable optical density filter; (ii): VCSEL; (iii): analysis branch; PD: photodiode, OSA: optical spectrum analyser. Reprinted from [76]



linear polarization of the injected light is tuned to match the one of the VCSEL. In order to produce LSs, both the optical injection power and the detuning between the injection frequency and the VCSEL resonance frequency are adjusted.

The VCSEL we use is a $80\mu\text{m}$ diameter, bottom emitting InGaAs multiple quantum well VCSEL, as described in Sec.(2) which has a threshold current of 42.5 mA at 25.0°C .

We analyse the optical spectrum, near field and output power of the VCSEL.

A photograph of the actual setup is shown in Fig.3.

3.2 Experimental observations

Tuning the width of the injection beam to $100\mu\text{m}$, the detuning to -174GHz , the VCSEL driving current to 45.013mA and its substrate temperature to 25.01°C , we obtain the bistability curve depicted in Fig. 4. We continuously varied the optical injection power by increasing it, before decreasing it. The hysteresis phenomenon associated with this experiment is evidenced in Fig.4a). The insets represent near field

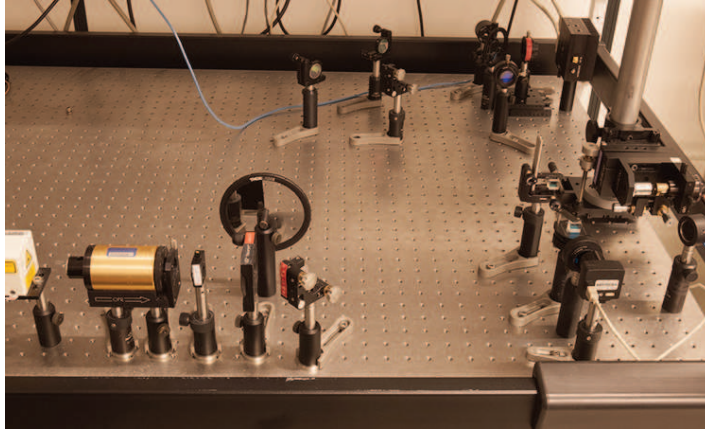


Fig. 3 Photography of the experimental setup. Left down side of the picture: injection preparation with external cavity laser diode, optical isolator, half-wave plate and variable optical density filter. Top right: injection monitoring and VCSEL. Down right: analysis branch; optical spectrum analyser, CCD camera and photodiode.

profiles on the higher and lower branch of the hysteresis curve. One dimensional profiles along the horizontal lines drawn on the insets are shown in Fig.4b)(up) and c)(down). The lower branch corresponds to the "homogeneous" steady state. In Fig.5, the difference between these two states is evidenced. On the higher branch, there is not only a peak, but a clearly noticeable oscillating tail around this peak, which is characteristic of a LS.

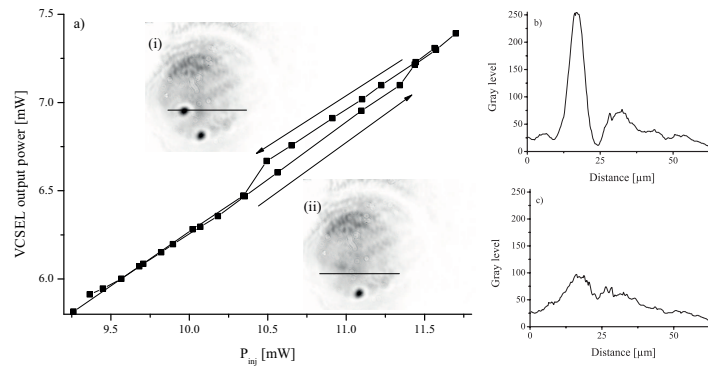


Fig. 4 Bistability between one and two-peaked LSs inside the near field of the VCSEL as a function of the optical injection power. (a): power emitted by the VCSEL as a function of the optical injection power for $\theta = -174\text{GHz}$ and a beam waist of $100\mu\text{m}$. The insets (i) and (ii) respectively represent near field profiles on the higher and lower branch of the hysteresis curve. (b) and (c): one dimensional profiles along the horizontal line drawn on the aforementioned insets. Redrawn from [76]

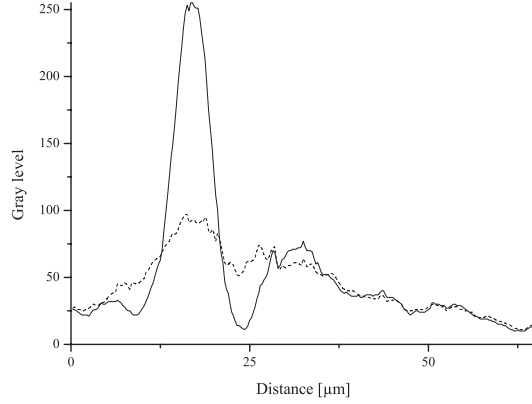


Fig. 5 Cross sections along the solid lines indicated in Fig.4(a), (i) and (ii). The dashed line is the state (ii)(lower branch of the hysteresis), whereas the full line is the system with a LS (upper branch of the hysteresis). Redrawn from [76]

4 Mean field model

In this section, we describe the dynamics of a VCSEL submitted to optical injection and delayed feedback. To do so, we assume an external cavity (i) in which the diffraction is compensated (ii) much longer than the characteristic diffraction length of the field. We further apply (i) a paraxial approximation (ii) a slowly varying envelope approximation. The mean field model describing the space-time evolution of the electric field envelope E and the carrier density N in a VCSEL subjected to optical injection and time-delayed feedback is then given by the following set of dimensionless partial differential equations

$$\frac{\partial E}{\partial t} = -(\mu + i\theta)E + 2C(1 - i\alpha)(N - 1)E + E_i - \eta e^{i\varphi}E(t - \tau) + i\nabla^2 E, \quad (1)$$

$$\frac{\partial N}{\partial t} = -\gamma \left[N - I + (N - 1)|E|^2 - d\nabla^2 N \right]. \quad (2)$$

The parameter α describes the linewidth enhancement factor, μ and θ are the cavity decay rate and the cavity detuning parameter, respectively. The parameter E_i is the amplitude of the injected field which we assume to be positive in order to fix the origin of the phase. C is the bistability parameter, γ is the carrier decay rate, I is the injection current, and d is the carrier diffusion coefficient. The light diffraction and the carrier diffusion are described by the terms $i\nabla^2 E$ and $d\nabla^2 N$, respectively, where ∇^2 is the Laplace operator acting in the transverse plane (x, y) . Below we consider the case when the laser is subjected to coherent delayed feedback from an external mirror. To minimize the effect of diffraction on the feedback field we assume that the external cavity is self-imaging [77]. The feedback is characterized by the delay time $\tau = 2L_{ext}/c$, the feedback rate $\eta \geq 0$, and phase φ , where L_{ext} is the

external cavity length, and c is the speed of light. The link between dimensionless and physical parameters is provided in [78]. Using the expression for the feedback rate $\eta = r^{1/2}(1-R)/R^{1/2}\tau_{in}$ given in [79], where $r(R)$ is the power reflectivity of the feedback (VCSEL top) mirror and τ_{in} is the VCSEL cavity round trip time, we see that the necessary condition for the appearance of the soliton drift instability $\eta\tau > 1$ [77] can be rewritten in the form $r > \frac{R\tau_{in}^2}{(1-R)^2\tau^2}$. In particular, for $R = 0.3$ and $\tau = 20\tau_{in}$ the latter inequality becomes $r > 1.5 \cdot 10^{-3}$.

To reduce the number of parameters, we introduce the following change of variables: $n = [2C(N-1) - 1]/2$ and $e = E^*/\sqrt{2}$. The model Eqs. (1,2) of a VCSEL driven by an injected field $Y = E_i/(2\sqrt{2})$ take the following form:

$$\partial_t e = i\theta' e + (1 + i\alpha)ne + Y + \eta' e^{-i\psi} e(t - \tau) - i\nabla^2 e, \quad (3)$$

$$\partial_t n = \gamma[P - n - (1 + 2n)|e|^2 + D\nabla^2 n]. \quad (4)$$

The pump parameter P is $P = C(I-1) - 1/2$, $\gamma = \gamma'/2$, $D = 2d$, $\eta' = \xi/2$, and $\theta' = (\theta + \alpha)/2$. The new time and space scales are $(t, \tau) = 2(t', \tau')$ and $\nabla_{\perp}^2 = 2\nabla_{\perp}'^2$. Let us assume for simplicity that the detuning is $\theta' = 0$ and the feedback phases are $\psi = 0$ or $\psi = \pi$.

The homogeneous steady states of Eqs. (3,4) are $Y = -e_s(1 + i\alpha)(P - |e_s|^2)/(1 + 2|e_s|^2)$ and $n_s = (P - |e_s|^2)/(1 + 2|e_s|^2)$. We explore the vicinity of the nascent optical bistability regime where there exists a second order critical point marking the onset of a hysteresis loop. The critical point associated with bistability is obtained when the output intensity as a function of the injection parameter Y has an infinite slope, i.e., $\partial Y/\partial |e_s| = \partial^2 Y/\partial |e_s|^2 = 0$. The coordinates of the critical point are $e_c = (1 - i\alpha)\sqrt{3/2(1 + \alpha^2)}$, $n_c = -3/2$, $P_c = -9/2$, $D_c = 8\alpha/[3(1 + \alpha^2)]$ and $Y_c = (3/2)^{(3/2)}(1 + \alpha^2)^{1/2}$. Our objective is to determine a slow time and slow space amplitude equation which is valid under the following approximations: (i) close to the onset of bistability (ii) close to large wavelength symmetry breaking instability. Starting from Eqs. (3, 4), the deviation u of the electric field from its value at the onset of bistability is shown to obey [80]

$$\begin{aligned} \partial_t u = & y - u(p + u^2) + \eta u(t - \tau) \\ & + (d - \frac{5u}{2})\nabla^2 u - a\nabla^4 u - 2(\nabla u)^2, \end{aligned} \quad (5)$$

where $a = (1 - \alpha^2)/(4\alpha^2)$. The parameter y denotes the deviation of the injected field amplitude from Y_c . The real variable u , the parameters p and d are the deviations of the electric field, the pump parameter and the carrier diffusion coefficient from their values at the onset of the critical point, respectively. In the absence of delay; i.e., $\eta = 0$, Eq.(5) is the generalized Swift-Hohenberg equation that has been derived for many far from equilibrium systems [81, 82, 83]. Even in absence of the delay feedback term, the terms $u\nabla^2 u$ and $(\nabla u)^2$ render Eq.(5) nonvariational.

5 Stationary localized structures

LSs are nonlinear bright or dark peaks in spatially extended systems. Such structures have been observed in the transverse section of coherently driven optical cavities, and are often called cavity solitons. Currently they attract growing interest in optics due to potential applications for all-optical control of light, optical storage, and information processing [2, 3]. When they are sufficiently separated from each other, localized peaks are independent and randomly distributed in space. However, when the distance between peaks decreases they start to interact via their oscillating, exponentially decaying tails. This interaction then leads to the formation of clusters [4, 5, 6, 7]. Mathematically speaking, LSs are homoclinic solutions (solitary or stationary pulses) of partial differential equations. The conditions under which LSs and periodic patterns appear are closely related. Typically, when the Turing instability becomes sub-critical, there exists a pinning domain where localized structures are stable. This is a universal phenomenon and a well documented issue in various fields of nonlinear science, such as chemistry, plant ecology, or optics (see some recent overviews on this multidisciplinary issue ([41, 42, 48])).

In this section we describe some basic properties of stationary LS and their bifurcation diagrams in a one dimensional setting. In the absence of delay feedback, Eq. (5) admits a variety of LSs. The generalized Swift-Hohenberg equation(5) is numerically integrated using a classical spatial finite-difference method with forward temporal Euler integration. The boundary conditions are periodic in both transverse directions and the initial condition consists of a large amplitude peaks added to the unstable homogeneous steady state. We fix all the parameters except the amplitude of the injected field y . Examples of localized clusters having an odd or an even number of peaks are shown in Figs. 1b and 1c. They are obtained for the same parameter values and differ only by the initial condition.

We examine the case of one-dimensional monostable system in the subcritical regime where the homogeneous steady state coexists with a spatially periodic structure. In addition, the system exhibits a high degree of multistability in a finite range of y values often called the pinning region [84]. More precisely, Eq. (5) then admits an infinite set of odd and even cavity solitons as shown in Fig. 6A, i.e., a set of stationary solutions that exhibit $n = 2p - 1$ or $n = 2p$ peaks, where p is a positive integer. The limit $p \rightarrow \infty$, corresponds to the infinitely extended periodic pattern distribution. In the pinning region, the width of LS is close to the half of the periodic wavelength structure. Since the amplitudes of localized patterns having different number of peaks are close to one another, in order to visualize the clusters properties, it is convenient to plot the “ L_2 -norm”

$$\mathcal{N} = \int dx dy |u - u_s|^2 \quad (6)$$

as a function of the injected field y . This yields the two snaking curves with odd or even number of peaks as shown in bifurcation diagram of Fig. (6B). As \mathcal{N} increases, at each turning point where the slope becomes infinite, a pair of additional

peaks appears in the cluster. One sees that this behavior, referred to as homoclinic snaking phenomenon [85, 86, 87, 88, 89, 90, 91], and recently observed experimentally [92, 93], corresponds to back and forth oscillations inside the pinning region. In two spatial dimensions, the variety of stable localized patterns is much larger than in one dimensional system.

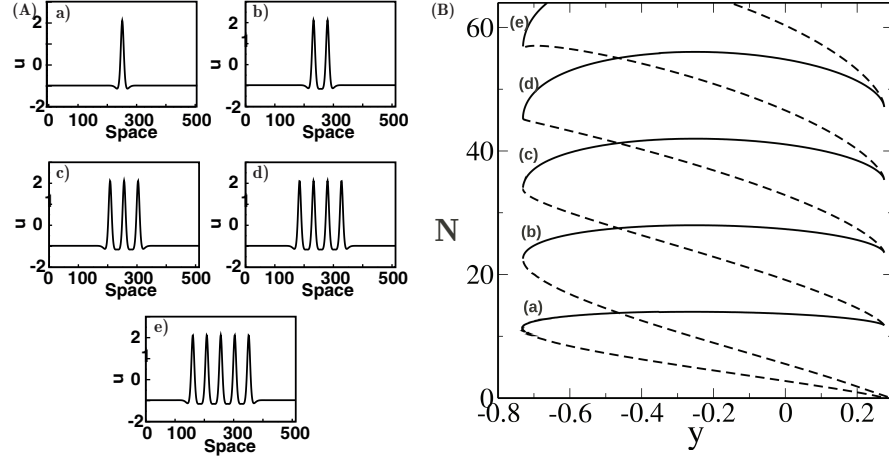


Fig. 6 One dimensional LSs. (A) Multiple peaks localized structures with odd or even number of peaks obtained for $y = -0.35$. (B) Snaking bifurcation diagram showing two inter-weaved snaking curves: the branches (a), (b), (c), (d) and (e) correspond to states having 1, 2, 3, 4 and 5 peaks in fig. 6A. Redrawn from [80]. The full and the broken lines correspond, respectively, to stable and unstable localized branches of LSs. The parameters are $p = -0.7$, $d = -1.2$, $a = 0.75$, and $\tau = \eta = 0$.

6 Moving localized structures

In this section we investigate the effect of a time-delayed feedback control on the stability of LSs in VCSELs. This delayed feedback loop compares the electric field at the current moment of time and its values at some time in the past. Recent studies that combined analytical and numerical analysis of the two-dimensional Swift–Hohenberg equation suggested that steady LSs can become mobile when $\eta\tau < 1$ [77, 94, 80].

$$v = \frac{Q}{\tau} \sqrt{-(1 - \eta\tau)}, \quad (7)$$

with

$$Q = \sqrt{6 \frac{\int_{-\infty}^{+\infty} u_1^2 dx dy}{\int_{-\infty}^{+\infty} u_2^2 dx dy}}$$

Due to the rotational symmetry of the generalized Swift-Hohenberg equation (5), there is no preferred direction for the motion of a circularly symmetric localized structure. The instability leading to the spontaneous motion of a LS solution is a circle pitchfork type of bifurcation. Therefore, the x axis can be chosen for the estimation of the velocity \mathbf{v} . In this case we obtain $u_1 = \partial u_0(\mathbf{r})/\partial x$ and $u_2 = \partial^2 u_0(\mathbf{r})/\partial x^2$ where $u_0(\mathbf{r})$ is the stationary localized structure solution. We recover the expression for the soliton velocity (7) that was obtained first in the case of the Swift-Hohenberg equation [77]. The speed formula (7) is valid for any localized pattern, regardless of the number of peaks it contains. The factor Q describes the spatial form of the localized pattern. This factor can be calculated only numerically. In particular, for the parameter values $y = -0.35$, $p = -0.7$, $d = -1.2$, $a = 0.75$, we obtain $Q = 1.44$. The velocity Eq. (7) divided by the factor Q is plotted as a function the delay time for a fixed value of the feedback strength as shown in Fig. 7. The curve of the velocity has a maximum at $\tau = 2/\eta$, which corresponds to the maximal velocity $v_{max} = Q\eta/2$. Note that the threshold $\eta\tau = 1$ and the expression for the formula (7) have been found later on for the chemical reaction-diffusion type of equations [95, 96, 97].

Numerical simulations of the Eq. (5) show indeed that single and many peaked LSs exhibit a spontaneous motion as predicted by the above theoretical analysis, as shown in Fig. 8.

The velocity and the threshold $\eta\tau = 1$ associated with the LS motion depend only on the delay parameters η and τ . This statement is valid only in nascent optical bistability regime, where the dynamics of the system are described by the real order parameter equation (5), and for a fixed feedback phase of $\psi = 0$ or $\psi = \pi$. In what follows we will examine the combined role of the phase of the delay feedback ψ and the carrier relaxation rate γ in the framework of the full mean field model.

Since our system is isotropic, the motion of localized structures occurs in an arbitrary direction. At the pitchfork bifurcation the stationary LS loses stability and a branch of moving LSs with the velocity $v = |\mathbf{v}|$ bifurcates from the stationary LS branch of solutions. The bifurcation point can be obtained from the first order expansion of the uniformly moving LS in power series of the small velocity v . Close to the bifurcation point, the uniformly moving LS can be expanded in power series in the small velocity v and through the solvability condition, we obtain the drift instability threshold [98, 99]

$$\eta\tau = \frac{1 + \gamma^{-1}(b/c)}{\sqrt{1 + (a/c)^2} \cos[\varphi + \arctan(a/c)]} \quad (8)$$

with

$$\begin{aligned} a &= \langle \psi_1^\dagger, \psi_2 \rangle - \langle \psi_2^\dagger, \psi_1 \rangle, \\ b &= \langle \psi_3^\dagger, \psi_3 \rangle, \\ c &= \langle \psi_1^\dagger, \psi_1 \rangle + \langle \psi_2^\dagger, \psi_2 \rangle, \end{aligned} \quad (9)$$

and

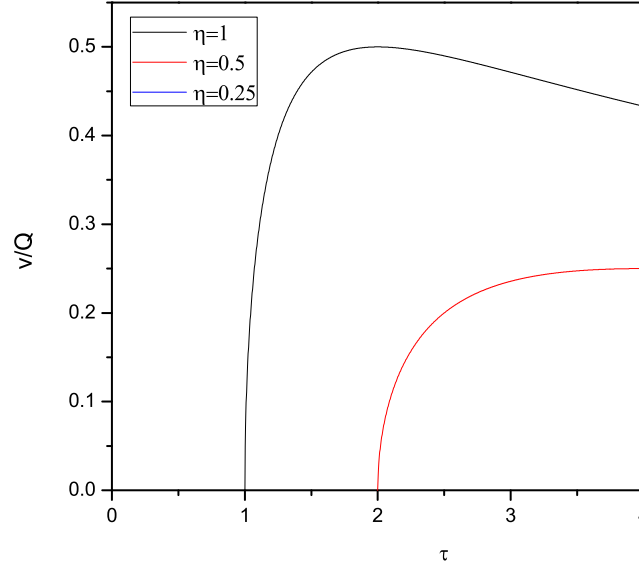


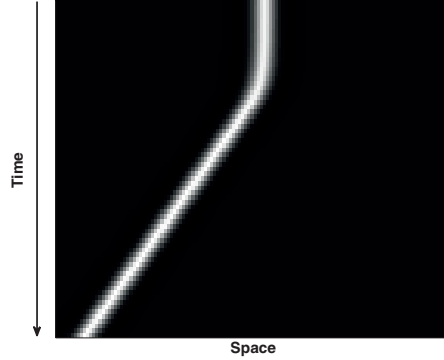
Fig. 7 Velocity by unit of the factor Q of moving localized structures as a function of the time delay τ for different values of the delayed feedback strength η .

$$\psi = (\psi_1, \psi_2, \psi_3)^T = \partial_x (X_0, Y_0, N_0)^T \quad (10)$$

a translational neutral mode of the linear operator L , $L\psi = 0$, while $\psi^\dagger = (\psi_1^\dagger, \psi_2^\dagger, \psi_3^\dagger)^T$ is the corresponding solution of the homogeneous adjoint problem $L^\dagger \psi^\dagger = 0$. The real $X_0(x, y)$ and the imaginary $Y_0(x, y)$ parts of the electric field E_0 and the carrier density $N_0(x, y)$ are the stationary axially symmetric LS profiles. They correspond to the time-independent solutions of Eqs. (1) and (2) with $\tau = 0$. The coefficients a and b are calculated numerically using the relaxation method in two transverse dimensions.

From the expression of the threshold associated with the drift instability Eq. (8), we see that the product $\eta\tau$ is not unity as in the case of the generalized Swift-Hohenberg equation, but depends strongly on the feedback phase φ and carrier relaxation rate γ . We plot in Fig. 9, the threshold η associated with the drift instability as a function of the phase of the delay feedback. The numbers on top of the different curves are the different values of the carrier decay rate γ . The carrier relaxation rate strongly affects the threshold associated with the drift instability as shown in Fig. 9. When we increase the carrier relaxation rate, the threshold associated with the moving LS gets higher. In addition, we see from Fig. 9 that, whatever the value of the carrier relaxation rate, the drift instability occurs only within the subinterval $(\varphi_{min} - \pi/2, \varphi_{min} + \pi/2)$ of the interval $(\varphi_{min} - \pi, \varphi_{min} + \pi)$, where $\varphi_{min} = -\arctan a$ is the delay feedback phase, corresponding to the lowest critical feedback rate $\eta_0^{min} = (1 + \gamma^{-1}b)/(\tau\sqrt{1+a^2})$. Note that when η_0 increases very rapidly when approaching the boundaries of these subintervals. In the limit of fast carrier response, $\gamma \gg 1$, and for zero feedback phase, $\varphi = 0$, we recover the expression (8), the threshold formula $\eta\tau = 1$ that has been obtained in both variational Swift-Hohenberg equation [77], and in a modified nonvariational one [80]. Note that at $\gamma \rightarrow \infty$, $a \neq 0$, and $\varphi = -\arctan a$ the critical feedback rate appears to be smaller than that obtained for the real Swift-Hohenberg equation, $\eta\tau = (1 + a^2)^{-1/2} < 1$.

Fig. 8 Space time map of a single-peaked localized structure solution to eq. (5). Parameters are $p = -0.9$, $d = -1.5$, $y = -0.5$, $\eta = 0.15$ and $\tau = 15$. Redrawn from Ref. [100]



To estimate the velocity of moving localized structure, we expand the slowly moving localized solution in the limit of a small velocity v . The detailed calculations can be found in [99]. The velocity v of LSs then obeys

$$v = \sqrt{\delta\eta}Q \text{ with } Q = (1/\tau)\sqrt{q/(r\eta)}. \quad (11)$$

The factor Q is important since it determines how fast the LS speed increases with the square root of the distance from the critical feedback rate. The Q factor depends on the delay feedback phase as shown Fig. 10. The $\delta\eta$ denotes the deviation of the feedback strength from the bifurcation point associated with the moving LS. The coefficients r and q are $q = a \sin \varphi + c \cos \varphi$, and $r = f \sin \varphi + g \cos \varphi + \mathcal{O}(\tau^{-1})$ with

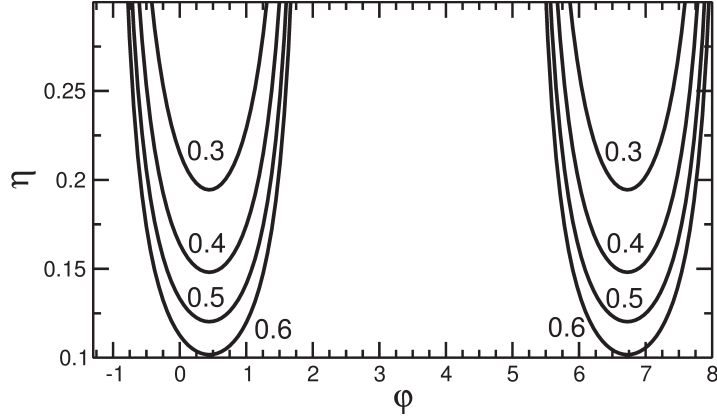


Fig. 9 Threshold associated with the drift bifurcation as a function of the feedback phase ϕ is plotted for different values of the carrier relaxation rate γ . Parameters are $\mu = 1.0$, $\theta = -2.0$, $C = 0.45$, $\alpha = 5.0$, $\tau = 100$, $d = 0.052$, $E_i = 0.8$, $I = 2$. The values of the parameter γ are shown in the figure. Redrawn from [99].

$f = \langle \psi_1^\dagger, \partial_{xxx} Y_0 \rangle - \langle \psi_2^\dagger, \partial_{xxx} X_0 \rangle$, $h = \langle \psi_3^\dagger, \partial_{xxx} N_0 \rangle$, $g = \langle \psi_1^\dagger, \partial_{xxx} X_0 \rangle + \langle \psi_2^\dagger, \partial_{xxx} Y_0 \rangle$. The coefficients a and c are defined in Eq. 10.

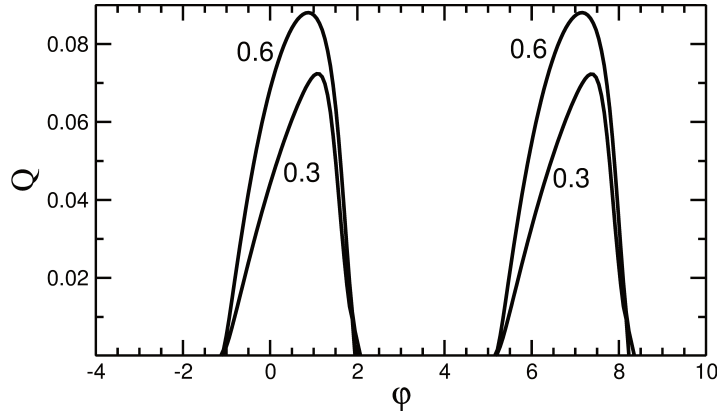


Fig. 10 Q factor as a function of the feedback phase ϕ , for different values of the carrier relaxation rate γ . The Q factor describes the growth rate of the LS velocity with the square root of the deviation from the critical feedback rate. Parameters are $\mu = 1.0$, $\theta = -2.0$, $C = 0.45$, $\alpha = 5.0$, $\tau = 100$, $d = 0.052$, $E_i = 0.8$, $I = 2$. The values of the parameter γ are shown in the figure. Redrawn from [99].

Numerical simulations of the full model Eqs. (1,2) and the generalized Swift-Hohenberg equation Eq. (5) agree with the above theoretical predictions. Indeed, when we choose parameter values such as the system operates above the threshold associated with the motion of LS, a single-peaked LS exhibits a regular motion in

the transverse plane of the cavity as shown in Fig. 8 (1-dimensional setting, (Eq.5)) and 11(2-dimensional setting, Eqs (1) and (2)).

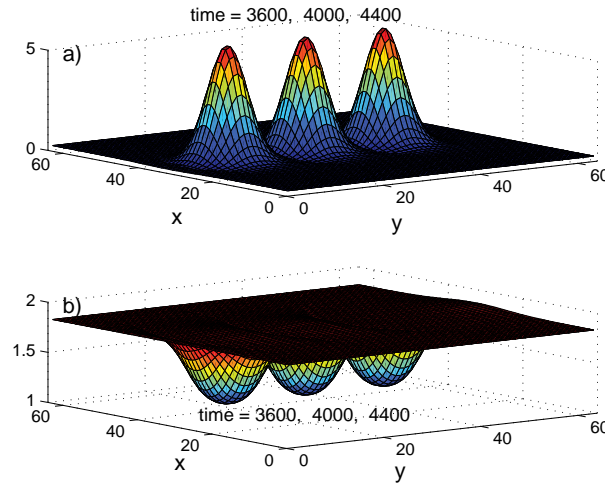


Fig. 11 Field intensity $|E|^2$ (top) and carrier density N (bottom) of a single peaked two-dimensional moving cavity soliton at different times. Parameters are $C = 0.45$, $\theta = -2$, $\alpha = 5$, $\gamma = 0.05$, $d = 0.052$, $\mu = 2$, $E_i = 0.8$, $\tau = 200$, $\eta = 0.07$, $\phi = 3.5$. Results obtained using Eqs. 1 and 2. Redrawn from [98].

Note, however, that the motion of LS under the effects of delay feedback is not always regular. It has been shown recently that LSs can exhibit a temporal chaos: numerical simulations of a broad area VCSEL with saturable absorber subjected to time-delayed optical feedback have shown evidence of complex temporal dynamics of LSs [101]. This spatio-temporal chaos is localized in space. More recently, in the absence of decay feedback, it has been shown that the VCSEL with saturable absorber without optical injection injection may exhibit LSs that drift and oscillate simultaneously, and a chaotic behavior [102, 103].

7 Conclusions and perspectives

In this chapter we have investigated the formation of localized structures in a Vertical-Cavity Surface-Emitting Laser subject to optical injection. This device consists of a medium size bottom-emitting InGaAs multiple quantum well VCSEL operating in an injection locked regime. In this regime, we have described experimentally the formation of stationary localized structures of light in the transverse section of this device. The experimental part has been performed in an injection

locked regime and in the absence of delay feedback control. We have characterized LSs by drawing their bifurcation diagram and performed a numerical simulation for the full model and the generalized Swift-Hohenberg equation.

Then we have described the space-time dynamics of a VCSEL by adding the delay feedback control in the modelling by adopting a mean-field approach. The time-delayed feedback is modelled following a Rosanov-Lang-Kobayashi approach [70, 71]. We have then analysed theoretically the effect of time delayed feedback from an external mirror on the stability of transverse localized structures in a broad area VCSEL. We have derived a real order parameter equation of the Swift-Hohenberg type with delay feedback. This analysis is only valid close the nascent optical bistability and close to large wavelength pattern forming regime. In this double limit, we have estimated the threshold associated with the drift-instability leading to the spontaneous motion of LS. Explicitly the threshold is given by a simple formula $\eta\tau = 1$. We conclude that the condition under which transition from motionless LS to a moving one, depends only on the delay feedback η and the delay time τ and not on the other dynamical parameters of the VCSEL system. This conclusion is valid for the variational and nonvariational Swift-Hohenberg equations, and in reaction-diffusion systems. However, in optics, the role of the phase is important because the intensity and the phase of the light operate on the same time scale. We have investigated in the last part of this chapter the role of the phase of the feedback on the mobility of LS. We have shown that, depending on the phase of the feedback, it can have either stabilizing or destabilizing effect on the LSs. In particular, when the interference between the LS field and the feedback field is destructive, the LS can be destabilized via a pitchfork bifurcation, where a branch of uniformly moving LS bifurcates from the stationary one. We have calculated analytically the threshold value of the feedback rate corresponding to this bifurcation and demonstrated that the faster the carrier relaxation rate in the semiconductor medium, the lower the threshold of the spontaneous drift instability induced by the feedback. This is a generic and robust destabilization mechanism in one and two spatial dimensions settings and could be applied to a large class of optical systems under time-delay control.

We have described spatially localized structures, recent investigations have shown that temporal localized structures have been found in fibre resonators [104, 90, 105, 106, 107, 108] and in VCSELS with a saturable absorber [109]. On the other hand, it has been shown that the combined influence of diffraction and chromatic dispersion leads to the formation of three dimensional localized structures often called light bullet [110, 111, 112, 113]. We plan in the future to investigate the effect of delayed feedback on the spontaneous motion of three dimensional light bullets.

In order to check our theoretical predictions, we also plan to investigate experimentally the formation of moving LS in VCSELS. In addition, we will analyse the role of local polarization dynamics in the formation of LSs in the transverse plane of the VCSEL. This would allow us to study the spontaneous motion of vector LSs with different polarizations under the effect of delayed feedback.

A.G.V. and A.P. acknowledge the support from SFB 787 of the DFG. A.G.V. acknowledges the support of the EU FP7 ITN PROPHET and E.T.S. Walton Visitors

Award of the Science Foundation Ireland. M.T. received support from the Fonds National de la Recherche Scientifique (Belgium). This research was supported in part by the Interuniversity Attraction Poles program of the Belgian Science Policy Office under Grant No. IAP P7-35.

References

1. L.A. Lugiato, R. Lefever, Phys. Rev. Lett. **58**, 2209 (1987). DOI 10.1103/PhysRevLett.58.2209. URL <http://link.aps.org/doi/10.1103/PhysRevLett.58.2209>
2. M. Tlidi, P. Mandel, R. Lefever, Phys. Rev. Lett. **73**, 640 (1994). DOI 10.1103/PhysRevLett.73.640. URL <http://link.aps.org/doi/10.1103/PhysRevLett.73.640>
3. A.J. Scroggie, W.J. Firth, G.S. McDonald, M. Tlidi, R. Lefever, L.A. Lugiato, Chaos, Solitons and Fractals **4**(8), 1323 (1994). DOI [http://dx.doi.org/10.1016/0960-0779\(94\)90084-1](http://dx.doi.org/10.1016/0960-0779(94)90084-1). URL <http://www.sciencedirect.com/science/article/pii/S0960077994900841>
4. A. Vladimirov, J. McSloy, D. Skryabin, W. Firth, Phys. Rev. E **65**, 046606 (2002). DOI 10.1103/PhysRevE.65.046606. URL <http://link.aps.org/doi/10.1103/PhysRevE.65.046606>
5. M. Tlidi, A.G. Vladimirov, P. Mandel, Quantum Electronics, IEEE Journal of **39**(2), 216 (2003). DOI 10.1109/JQE.2002.807193
6. M. Tlidi, R. Lefever, A. Vladimirov, Lecture notes in Physics **751**, 381 (2008)
7. D. Turaev, A.G. Vladimirov, S. Zelik, Phys. Rev. Lett. **108**, 263906 (2012). DOI 10.1103/PhysRevLett.108.263906. URL <http://link.aps.org/doi/10.1103/PhysRevLett.108.263906>
8. S. Fauve, O. Thual, Phys. Rev. Lett. **64**, 282 (1990). DOI 10.1103/PhysRevLett.64.282. URL <http://link.aps.org/doi/10.1103/PhysRevLett.64.282>
9. N.N. Rosanov, in *Progress in Optics, Progress in Optics*, vol. 35, ed. by E. Wolf (Elsevier, 1996), pp. 1 – 60. DOI [http://dx.doi.org/10.1016/S0079-6638\(08\)70527-4](http://dx.doi.org/10.1016/S0079-6638(08)70527-4). URL <http://www.sciencedirect.com/science/article/pii/S0079663808705274>
10. G. Sleky, K. Staliunas, C. Weiss, Optics Communications **149**(1–3), 113 (1998). DOI [http://dx.doi.org/10.1016/S0030-4018\(97\)00667-6](http://dx.doi.org/10.1016/S0030-4018(97)00667-6). URL <http://www.sciencedirect.com/science/article/pii/S0030401897006676>
11. A.G. Vladimirov, D.V. Skryabin, G. Kozyreff, P. Mandel, M. Tlidi, Opt. Express **14**(1), 1 (2006). DOI 10.1364/OPEX.14.000001. URL <http://www.opticsexpress.org/abstract.cfm?URI=oe-14-1-1>
12. K. Staliunas, V.J. Sánchez-Morcillo, Optics Communications **139**(4–6), 306 (1997). DOI [http://dx.doi.org/10.1016/S0030-4018\(97\)00109-0](http://dx.doi.org/10.1016/S0030-4018(97)00109-0). URL <http://www.sciencedirect.com/science/article/pii/S0030401897001090>
13. S. Longhi, Opt. Lett. **23**(5), 346 (1998). DOI 10.1364/OL.23.000346. URL <http://ol.osa.org/abstract.cfm?URI=ol-23-5-346>
14. P. Kockaert, P. Tassin, G. Van der Sande, I. Veretennicoff, M. Tlidi, Phys. Rev. A **74**, 033822 (2006). DOI 10.1103/PhysRevA.74.033822. URL <http://link.aps.org/doi/10.1103/PhysRevA.74.033822>
15. L. Gelens, G. Van der Sande, P. Tassin, M. Tlidi, P. Kockaert, D. Gomila, I. Veretennicoff, J. Danckaert, Phys. Rev. A **75**, 063812 (2007). DOI 10.1103/PhysRevA.75.063812. URL <http://link.aps.org/doi/10.1103/PhysRevA.75.063812>
16. A.B. Kozyrev, I.V. Shadrivov, Y.S. Kivshar, Applied Physics Letters **104**(8), 084105 (2014). DOI <http://dx.doi.org/10.1063/1.4866856>. URL <http://scitation.aip.org/content/aip/journal/apl/104/8/10.1063/1.4866856>
17. M. Tlidi, P. Kockaert, L. Gelens, Phys. Rev. A **84**, 013807 (2011). DOI 10.1103/PhysRevA.84.013807. URL <http://link.aps.org/doi/10.1103/PhysRevA.84.013807>

18. A. Werner, O.A. Egorov, F. Lederer, Phys. Rev. B **90**, 165308 (2014). DOI 10.1103/PhysRevB.90.165308. URL <http://link.aps.org/doi/10.1103/PhysRevB.90.165308>
19. A. Werner, O.A. Egorov, F. Lederer, Phys. Rev. B **89**, 245307 (2014). DOI 10.1103/PhysRevB.89.245307. URL <http://link.aps.org/doi/10.1103/PhysRevB.89.245307>
20. H. Brand, R. Deissler, Phys. Rev. Lett. **63**, 2801 (1989). DOI 10.1103/PhysRevLett.63.2801. URL <http://link.aps.org/doi/10.1103/PhysRevLett.63.2801>
21. B. Malomed, Phys. Rev. A **44**, 6954 (1991). DOI 10.1103/PhysRevA.44.6954. URL <http://link.aps.org/doi/10.1103/PhysRevA.44.6954>
22. B. Malomed, Phys. Rev. E **58**, 7928 (1998). DOI 10.1103/PhysRevE.58.7928. URL <http://link.aps.org/doi/10.1103/PhysRevE.58.7928>
23. V. Besse, H. Leblond, D. Mihalache, B. Malomed, Phys. Rev. E **87**, 012916 (2013). DOI 10.1103/PhysRevE.87.012916. URL <http://link.aps.org/doi/10.1103/PhysRevE.87.012916>
24. V. Skarka, N.B. Aleksić, M. Lekić, B.N. Aleksić, B.A. Malomed, D. Mihalache, H. Leblond, Phys. Rev. A **90**, 023845 (2014). DOI 10.1103/PhysRevA.90.023845. URL <http://link.aps.org/doi/10.1103/PhysRevA.90.023845>
25. K. Staliunas, V.J. Sánchez-Morcillo, Physics Letters A **241**(1–2), 28 (1998). DOI [http://dx.doi.org/10.1016/S0375-9601\(98\)00084-X](http://dx.doi.org/10.1016/S0375-9601(98)00084-X). URL <http://www.sciencedirect.com/science/article/pii/S037596019800084X>
26. M. Tlidi, P. Mandel, R. Lefever, Phys. Rev. Lett. **81**, 979 (1998)
27. M. Tlidi, P. Mandel, M.L. Berre, E. Ressayre, A. Tallet, L.D. Menza, Opt. Lett. **25**(7), 487 (2000). DOI 10.1364/OL.25.000487. URL <http://ol.osa.org/abstract.cfm?URI=ol-25-7-487>
28. G. Izús, M. San Miguel, M. Santagiustina, Phys. Rev. E **64**, 056231 (2001). DOI 10.1103/PhysRevE.64.056231. URL <http://link.aps.org/doi/10.1103/PhysRevE.64.056231>
29. C. Fernandez-Oto, G.J. de Valcárcel, M. Tlidi, K. Panajotov, K. Staliunas, Phys. Rev. A **89**, 055802 (2014). DOI 10.1103/PhysRevA.89.055802. URL <http://link.aps.org/doi/10.1103/PhysRevA.89.055802>
30. C. Fernandez-Oto, M. Clerc, D. Escaff, M. Tlidi, Phys. Rev. Lett. **110**, 174101 (2013). DOI 10.1103/PhysRevLett.110.174101. URL <http://link.aps.org/doi/10.1103/PhysRevLett.110.174101>
31. L.A. Lugiato, Chaos, Solitons and Fractals **4**, 1251 (1994). DOI [http://dx.doi.org/10.1016/0960-0779\(94\)90080-9](http://dx.doi.org/10.1016/0960-0779(94)90080-9). URL <http://www.sciencedirect.com/science/article/pii/0960077994900809>. Special Issue: Nonlinear Optical Structures, Patterns, Chaos;ce:title;
32. P. Mandel, *Theoretical Problems in Cavity Nonlinear Optics* (Cambridge University Press, 1997). URL <http://dx.doi.org/10.1017/CBO9780511529337>. Cambridge Books Online
33. F. Arecchi, S. Boccaletti, P. Ramazza, Physics Reports **318**(1–2), 1 (1999). DOI [http://dx.doi.org/10.1016/S0370-1573\(99\)00007-1](http://dx.doi.org/10.1016/S0370-1573(99)00007-1). URL <http://www.sciencedirect.com/science/article/pii/S0370157399000071>
34. L.M. Pismen, *Vortices in Nonlinear Fields: From Liquid Crystals to Superfluids, from Non-equilibrium Patterns to Cosmic Strings, International series of monographs on physics*, vol. 100, clarendon press edn. (Oxford University Press, 1999)
35. N.N. Rosanov, *Spatial Hysteresis and Optical Patterns*. Springer Series in Synergetics (Springer Berlin Heidelberg, 2002). DOI 10.1007/978-3-662-04792-7. URL <http://dx.doi.org/10.1007/978-3-662-04792-7>
36. K. Staliunas, V. Sánchez-Morcillo, *Transverse Patterns in Nonlinear Optical Resonators*. Springer tracts in modern physics (Springer Berlin Heidelberg, 2003). DOI 10.1007/3-540-36416-1. URL <http://dx.doi.org/10.1007/3-540-36416-1>

37. Y.S. Kivshar, G.P. Agrawal, *Optical Solitons: From Fibers to Photonic Crystals* (Elsevier, 2003). URL <http://www.sciencedirect.com/science/book/9780124105904>
38. C. Denz, M. Schwab, C. Weillnau, *Transverse-Pattern Formation in Photorefractive Optics, Springer Tracts in Modern Physics*, vol. 188 (Springer Berlin Heidelberg, 2003). DOI 10.1007/b13583. URL <http://dx.doi.org/10.1007/b13583>
39. P. Mandel, M. Tlidi, *Journal of Optics B: Quantum and Semiclassical Optics* **6**(9), R60 (2004). URL <http://stacks.iop.org/1464-4266/6/i=9/a=R02>
40. B.A. Malomed, D. Mihalache, F. Wise, L. Torner, *Journal of Optics B: Quantum and Semiclassical Optics* **7**(5), R53 (2005). URL <http://stacks.iop.org/1464-4266/7/i=5/a=R02>
41. M. Tlidi, M. Taki, T. Kolokolnikov, *Chaos: An Interdisciplinary Journal of Nonlinear Science* **17**(3), 037101 (2007)
42. N. Akhmediev, A. Ankiewicz (eds.), *Dissipative Solitons: from Optics to Biology and Medicine, Lecture Notes in Physics*, vol. 751 (Springer, 2008)
43. T. Ackemann, W.J. Firth, G.L. Oppo, in *Advances In Atomic, Molecular, and Optical Physics, Advances In Atomic, Molecular, and Optical Physics*, vol. 57, ed. by P.R.B. E. Arimondo, C.C. Lin (Academic Press, 2009), chap. 6, p. 323. DOI [http://dx.doi.org/10.1016/S1049-250X\(09\)57006-1](http://dx.doi.org/10.1016/S1049-250X(09)57006-1). URL <http://www.sciencedirect.com/science/article/pii/S1049250X09570061>
44. R. Kuszelewicz, S. Barbay, G. Tissoni, G. Almuneau, *Eur. Phys. J. D* **59**(1), 1 (2010). DOI 10.1140/epjd/e2010-00167-7. URL <http://dx.doi.org/10.1140/epjd/e2010-00167-7>
45. H.G. Purwins, H.U. Bödeker, S. Amiranashvili, *Advances in Physics* **59**(5), 485 (2010). DOI 10.1080/00018732.2010.498228. URL <http://www.tandfonline.com/doi/abs/10.1080/00018732.2010.498228>
46. O. Descalzi, M. Clerc, S. Residori, *Localized States in Physics: Solitons and Patterns* (Springer, 2011). URL <http://books.google.be/books?id=PWJLOKeeAQIC>
47. H. Leblond, D. Mihalache, *Physics Reports* **523**(2), 61 (2013). DOI <http://dx.doi.org/10.1016/j.physrep.2012.10.006>. URL <http://www.sciencedirect.com/science/article/pii/S0370157312003511>
48. M. Tlidi, K. Staliunas, K. Panajotov, A.G. Vladimirov, M.G. Clerc, *Philosophical Transactions of the Royal Society of London A: Mathematical, Physical and Engineering Sciences* **372**, 20140101 (2014)
49. V.B. Taranenko, I. Ganne, R.J. Kuszelewicz, C.O. Weiss, *Phys. Rev. A* **61**, 063818 (2000). DOI 10.1103/PhysRevA.61.063818. URL <http://link.aps.org/doi/10.1103/PhysRevA.61.063818>
50. F. Pedaci, G. Tissoni, S. Barland, M. Giudici, J. Tredicce, *Appl. Phys. Lett.* **93**(11), 111104 (2008). DOI 10.1063/1.2977603. URL <http://link.aip.org/link/?APL/93/111104/1>
51. S. Barland, J.R. Tredicce, M. Brambilla, L.A. Lugiato, S. Balle, M. Giudici, T. Maggipinto, L. Spinelli, G. Tissoni, T. Knödl, et al., *Nature* **419**(6908), 699 (2002)
52. X. Hachair, F. Pedaci, E. Caboche, S. Barland, M. Giudici, J.R. Tredicce, F. Prati, G. Tissoni, R. Kheradmand, L.A. Lugiato, I. Protsenko, M. Brambilla, *Selected Topics in Quantum Electronics, IEEE Journal of* **12**(3), 339 (2006). DOI 10.1109/JSTQE.2006.872711
53. X. Hachair, G. Tissoni, H. Thienpont, K. Panajotov, *Phys. Rev. A* **79**, 011801 (2009). DOI 10.1103/PhysRevA.79.011801. URL <http://link.aps.org/doi/10.1103/PhysRevA.79.011801>
54. Y. Tanguy, T. Ackemann, W.J. Firth, R. Jäger, *Phys. Rev. Lett.* **100**, 013907 (2008). DOI 10.1103/PhysRevLett.100.013907. URL <http://link.aps.org/doi/10.1103/PhysRevLett.100.013907>
55. P.V. Paulau, D. Gomila, T. Ackemann, N.A. Loiko, W.J. Firth, *Phys. Rev. E* **78**, 016212 (2008). DOI 10.1103/PhysRevE.78.016212. URL <http://link.aps.org/doi/10.1103/PhysRevE.78.016212>

56. P. Genevet, S. Barland, M. Giudici, J.R. Tredicce, *Phys. Rev. Lett.* **101**, 123905 (2008). DOI 10.1103/PhysRevLett.101.123905. URL <http://link.aps.org/doi/10.1103/PhysRevLett.101.123905>
57. L. Columbo, F. Prati, M. Brambilla, T. Maggipinto, *The European Physical Journal D* **59**(1), 115 (2010). DOI 10.1140/epjd/e2010-00110-0. URL <http://dx.doi.org/10.1140/epjd/e2010-00110-0>
58. N.N. Rosanov, G.V. Khodova, *Optics and Spectroscopy* **65**, 449 (1988)
59. A.G. Vladimirov, S.V. Fedorov, N.A. Kaliteevskii, G.V. Khodova, N.N. Rosanov, *Journal of Optics B: Quantum and Semiclassical Optics* **1**(1), 101 (1999). URL <http://stacks.iop.org/1464-4266/1/i=1/a=019>
60. S.V. Fedorov, A.G. Vladimirov, G.V. Khodova, N.N. Rosanov, *Phys. Rev. E* **61**, 5814 (2000). DOI 10.1103/PhysRevE.61.5814. URL <http://link.aps.org/doi/10.1103/PhysRevE.61.5814>
61. T. Elsass, K. Gauthron, G. Beaudoin, I. Sagnes, R. Kuszelewicz, S. Barbay, *The European Physical Journal D* **59**(1), 91 (2010). DOI 10.1140/epjd/e2010-00079-6. URL <http://dx.doi.org/10.1140/epjd/e2010-00079-6>
62. T. Elsass, K. Gauthron, G. Beaudoin, I. Sagnes, R. Kuszelewicz, S. Barbay, *Applied Physics B* **98**(2-3), 327 (2010). DOI 10.1007/s00340-009-3748-9. URL <http://dx.doi.org/10.1007/s00340-009-3748-9>
63. F. Pedaci, P. Genevet, S. Barland, M. Giudici, J.R. Tredicce, *Applied Physics Letters* **89**(22), 221111 (2006). DOI <http://dx.doi.org/10.1063/1.2388867>. URL <http://scitation.aip.org/content/aip/journal/apl/89/22/10.1063/1.2388867>
64. F. Pedaci, S. Barland, E. Caboche, P. Genevet, M. Giudici, J.R. Tredicce, T. Ackemann, A.J. Scroggie, W.J. Firth, G.L. Oppo, G. Tissoni, R. Jäger, *Appl. Phys. Lett.* **92**(1), 011101 (2008). DOI 10.1063/1.2828458. URL <http://link.aip.org/link/?APL/92/011101/1>
65. H. Soda, K. Ichi Iga, C. Kitahara, Y. Suematsu, *Japanese Journal of Applied Physics* **18**(12), 2329 (1979). URL <http://stacks.iop.org/1347-4065/18/i=12/a=2329>
66. H.E. Li, K. Iga (eds.), *Vertical-Cavity Surface-Emitting Laser Devices, Springer Series in Photonics*, vol. 6 (Springer Berlin Heidelberg, 2003)
67. R. Michalzik (ed.), *VCSELs: Fundamentals, Technology and Applications of Vertical-Cavity Surface-Emitting Lasers, Springer Series in Optical Sciences*, vol. 166 (Springer Berlin Heidelberg, 2013)
68. K. Panajotov, M. Sciamanna, M. Arteaga, H. Thienpont, *Selected Topics in Quantum Electronics, IEEE Journal of* **19**(4), 1700312 (2013). DOI 10.1109/JSTQE.2012.2235060
69. K. Panajotov, I. Gatara, A. Valle, H. Thienpont, M. Sciamanna, *Quantum Electronics, IEEE Journal of* **45**(11), 1473 (2009). DOI 10.1109/JQE.2009.2024958
70. N. Rosanov, *Sov. J. Quantum Electronics* **10**, 1191 (1975)
71. K.K. R Lang, *Quantum Electronics, IEEE Journal of* **16**, 347 (1980)
72. K. Iga, *Japanese Journal of Applied Physics* **47**(1R), 1 (2008). URL <http://stacks.iop.org/1347-4065/47/i=1R/a=1>
73. K. Iga, *Selected Topics in Quantum Electronics, IEEE Journal of* **6**(6), 1201 (2000). DOI 10.1109/2944.902168
74. R. Michalzik, in *VCSELs, Springer Series in Optical Sciences*, vol. 166, ed. by R. Michalzik (Springer Berlin Heidelberg, 2013), pp. 3–18. DOI 10.1007/978-3-642-24986-0_1. URL http://dx.doi.org/10.1007/978-3-642-24986-0_1
75. M. Grabherr, M. Miller, R. Jager, R. Michalzik, U. Martin, H.J. Unold, K.J. Ebeling, *Selected Topics in Quantum Electronics, IEEE Journal of* **5**(3), 495 (1999). DOI 10.1109/2944.788411
76. E. Averlant, M. Tlidi, H. Thienpont, T. Ackemann, K. Panajotov, *Opt. Express* **22**(1), 762 (2014). DOI 10.1364/OE.22.000762. URL <http://www.opticsexpress.org/abstract.cfm?URI=oe-22-1-762>
77. M. Tlidi, A.G. Vladimirov, D. Pieroux, D. Turaev, *Phys. Rev. Lett.* **103**, 103904 (2009). DOI 10.1103/PhysRevLett.103.103904. URL <http://link.aps.org/doi/10.1103/PhysRevLett.103.103904>

78. K. Panajotov, M. Tlidi, *The European Physical Journal D* **59**(1), 67 (2010). DOI 10.1140/epjd/e2010-00111-y. URL <http://dx.doi.org/10.1140/epjd/e2010-00111-y>
79. G.H.M. van Tartwijk, D. Lenstra, *Quantum and Semiclassical Optics: Journal of the European Optical Society Part B* **7**(2), 87 (1995). URL <http://stacks.iop.org/1355-5111/7/i=2/a=003>
80. M. Tlidi, E. Averlant, A. Vladimirov, K. Panajotov, *Phys. Rev. A* **86**, 033822 (2012). DOI 10.1103/PhysRevA.86.033822. URL <http://link.aps.org/doi/10.1103/PhysRevA.86.033822>
81. G. Kozyreff, S. Chapman, M. Tlidi, *Phys. Rev. E* **68**, 015201 (2003). DOI 10.1103/PhysRevE.68.015201. URL <http://link.aps.org/doi/10.1103/PhysRevE.68.015201>
82. G. Kozyreff, M. Tlidi, *Chaos: An Interdisciplinary Journal of Nonlinear Science* **17**(3), 037103 (2007). DOI <http://dx.doi.org/10.1063/1.2759436>. URL <http://scitation.aip.org/content/aip/journal/chaos/17/3/10.1063/1.2759436>
83. M.G. Clerc, D. Escaff, V.M. Kenkre, *Phys. Rev. E* **72**, 056217 (2005). DOI 10.1103/PhysRevE.72.056217. URL <http://link.aps.org/doi/10.1103/PhysRevE.72.056217>
84. Y. Pomeau, *Physica D: Nonlinear Phenomena* **23**(1-3), 3 (1986). DOI [http://dx.doi.org/10.1016/0167-2789\(86\)90104-1](http://dx.doi.org/10.1016/0167-2789(86)90104-1). URL <http://www.sciencedirect.com/science/article/pii/0167278986901041>
85. A. Champneys, *Physica D: Nonlinear Phenomena* **112**(1-2), 158 (1998). DOI [http://dx.doi.org/10.1016/S0167-2789\(97\)00209-1](http://dx.doi.org/10.1016/S0167-2789(97)00209-1). URL <http://www.sciencedirect.com/science/article/pii/S0167278997002091>. Proceedings of the Workshop on Time-Reversal Symmetry in Dynamical Systems
86. P. Couillet, C. Riera, C. Tresser, *Phys. Rev. Lett.* **84**, 3069 (2000). DOI 10.1103/PhysRevLett.84.3069. URL <http://link.aps.org/doi/10.1103/PhysRevLett.84.3069>
87. M.G. Clerc, C. Falcon, E. Tirapegui, *Phys. Rev. Lett.* **94**, 148302 (2005). DOI 10.1103/PhysRevLett.94.148302. URL <http://link.aps.org/doi/10.1103/PhysRevLett.94.148302>
88. J. Burke, E. Knobloch, *Phys. Rev. E* **73**, 056211 (2006). DOI 10.1103/PhysRevE.73.056211. URL <http://link.aps.org/doi/10.1103/PhysRevE.73.056211>
89. J. Burke, E. Knobloch, *Chaos: An Interdisciplinary Journal of Nonlinear Science* **17**(3), 037102 (2007). DOI <http://dx.doi.org/10.1063/1.2746816>. URL <http://scitation.aip.org/content/aip/journal/chaos/17/3/10.1063/1.2746816>
90. M. Tlidi, L. Gelens, *Opt. Lett.* **35**(3), 306 (2010). DOI 10.1364/OL.35.000306. URL <http://ol.osa.org/abstract.cfm?URI=ol-35-3-306>
91. A.G. Vladimirov, R. Lefever, M. Tlidi, *Phys. Rev. A* **84**, 043848 (2011). DOI 10.1103/PhysRevA.84.043848. URL <http://link.aps.org/doi/10.1103/PhysRevA.84.043848>
92. F. Haudin, R. Rojas, U. Bortolozzo, S. Residori, M. Clerc, *Phys. Rev. Lett.* **107**, 264101 (2011). DOI 10.1103/PhysRevLett.107.264101. URL <http://link.aps.org/doi/10.1103/PhysRevLett.107.264101>
93. S. Barbay, X. Hachair, T. Elsass, I. Sagnes, R. Kuszelewicz, *Phys. Rev. Lett.* **101**, 253902 (2008). DOI 10.1103/PhysRevLett.101.253902. URL <http://link.aps.org/doi/10.1103/PhysRevLett.101.253902>
94. M. Tlidi, A.G. Vladimirov, D. Turaev, G. Kozyreff, D. Pieroux, T. Erneux, *The European Physical Journal D* **59**(1), 59 (2010). DOI 10.1140/epjd/e2010-00144-2. URL <http://dx.doi.org/10.1140/epjd/e2010-00144-2>
95. M. Tlidi, A. Sonnino, G. Sonnino, *Phys. Rev. E* **87**, 042918 (2013). DOI 10.1103/PhysRevE.87.042918. URL <http://link.aps.org/doi/10.1103/PhysRevE.87.042918>
96. S.V. Gurevich, *Phys. Rev. E* **87**, 052922 (2013). DOI 10.1103/PhysRevE.87.052922. URL <http://link.aps.org/doi/10.1103/PhysRevE.87.052922>

97. S. Gurevich, *Philos. Trans. R. Soc. Lond. A* (2014)
98. A. Pimenov, A.G. Vladimirov, S.V. Gurevich, K. Panajotov, G. Huyet, M. Tlidi, *Phys. Rev. A* **88**, 053830 (2013). DOI 10.1103/PhysRevA.88.053830. URL <http://link.aps.org/doi/10.1103/PhysRevA.88.053830>
99. A.G. Vladimirov, A. Pimenov, S.V. Gurevich, K. Panajotov, E. Averlant, M. Tlidi, *Philosophical Transactions of the Royal Society of London A: Mathematical, Physical and Engineering Sciences* **372**(2027) (2014). DOI 10.1098/rsta.2014.0013
100. E. Averlant, M. Tlidi, A.G. Vladimirov, H. Thienpont, K. Panajotov, in *Semiconductor Lasers and Laser Dynamics V*, vol. 8432 (2012), vol. 8432, p. 84321D. DOI 10.1117/12.921867. URL <http://dx.doi.org/10.1117/12.921867>
101. K. Panajotov, M. Tlidi, *Opt. Lett.* **39**(16), 4739 (2014). DOI 10.1364/OL.39.004739. URL <http://ol.osa.org/abstract.cfm?URI=ol-39-16-4739>
102. F. Prati, G. Tissoni, L.A. Lugiato, K.M. Aghdami, M. Brambilla, *The European Physical Journal D* **59**(1), 73 (2010). DOI 10.1140/epjd/e2010-00123-7
103. H. Vahed, F. Prati, M. Turconi, S. Barland, G. Tissoni, *Philosophical Transactions of the Royal Society of London A: Mathematical, Physical and Engineering Sciences* **372**(2027) (2014). DOI 10.1098/rsta.2014.0016
104. F. Leo, S. Coen, P. Kockaert, S.P. Gorza, P. Emplit, M. Haelterman, *Nat Photon* **4**, 471 (2010). DOI 10.1038/nphoton.2010.120
105. M. Tlidi, L. Bahloul, L. Cherbi, A. Hariz, S. Coulibaly, *Phys. Rev. A* **88**, 035802 (2013). DOI 10.1103/PhysRevA.88.035802. URL <http://link.aps.org/doi/10.1103/PhysRevA.88.035802>
106. M.J. Schmidberger, D. Novoa, F. Biancalana, P.S. Russell, N.Y. Joly, *Opt. Express* **22**(3), 3045 (2014). DOI 10.1364/OE.22.003045. URL <http://www.opticsexpress.org/abstract.cfm?URI=oe-22-3-3045>
107. C. Milián, D. Skryabin, *Opt. Express* **22**(3), 3732 (2014). DOI 10.1364/OE.22.003732. URL <http://www.opticsexpress.org/abstract.cfm?URI=oe-22-3-3732>
108. L. Bahloul, L. Cherbi, A. Hariz, M. Tlidi, *Philosophical Transactions of the Royal Society of London A: Mathematical, Physical and Engineering Sciences* **372**(2027) (2014). DOI 10.1098/rsta.2014.0020
109. M. Marconi, J. Javaloyes, S. Balle, M. Giudici, *Phys. Rev. Lett.* **112**, 223901 (2014). DOI 10.1103/PhysRevLett.112.223901. URL <http://link.aps.org/doi/10.1103/PhysRevLett.112.223901>
110. M. Tlidi, *Journal of Optics B: Quantum and Semiclassical Optics* **2**(3), 438 (2000). URL <http://stacks.iop.org/1464-4266/2/i=3/a=335>
111. M. Tlidi, M. Haelterman, P. Mandel, *Quantum and Semiclassical Optics: Journal of the European Optical Society Part B* **10**(6), 869 (1998). URL <http://stacks.iop.org/1355-5111/10/i=6/a=018>
112. N. Veretenov, M. Tlidi, *Phys. Rev. A* **80**, 023822 (2009). DOI 10.1103/PhysRevA.80.023822. URL <http://link.aps.org/doi/10.1103/PhysRevA.80.023822>
113. C.Q. Dai, X.G. Wang, G.Q. Zhou, *Phys. Rev. A* **89**, 013834 (2014). DOI 10.1103/PhysRevA.89.013834. URL <http://link.aps.org/doi/10.1103/PhysRevA.89.013834>